Monitoring Temporal Urban Expansion and Its Effect on LST Using Landsat Imagery

Sadeepta Dhungana[1], Dr. Niraj KC[2*]

[1] Department of Geomatics Engineering, Pashchimanchal Campus, Institute of Engineering, Tribhuvan University, Pokhara, Nepal

[2] Lumbini Technological University, Nepalgunj, Nepal

* dean.niraj@ltu.edu.np

(Manuscript Received: 18th January, 2026; Revised: 24th February, 2026; Accepted: 28th February, 2026)

Abstract

Nepal is one of the fastest urbanizing nations in South East Asia. Nepal's terai region has been facing huge pressure of urbanization due to rising population and rapid migration of people from hilly region to flat low lands. Bharatpur metropolitan city lies in Chitwan Nepal. The fertile lands of Bharatpur has been depleted to adjust the growing urban areas. This study assess the physical expansion of urban areas in Bharatpur Metropolitan City using Landsat imageries from years 2000, 2010 and 2020 and its effect on Land Surface Temperature. The Land Use/ Land Cover map revealed that there was massive increase of the built up area in the region in the period of 20 years. The built up area increased from 1.53 km^2 in 2000 to 30.02 km^2 in 2020. It has outgrown from urban core to extremity of the metropolitan city. By integrating temporal Land Use Land Cover (LULC) data with Shannon's Entropy, it is confirmed that the expansion of the built up area is highly disorganized. The Relative Shannon's Entropy value has rose from 0.56 to 0.88 in 2020, categorizing expansion of Bharatpur as "Extreme Sprawl". Built up areas consistently recorded the highest mean temperature across all three temporal periods. The conversion of natural land into heat retaining impervious surface has significantly changed the thermal pattern of the city.

Keywords: LST, LULC, Shannon's Entropy, Urban Sprawl,

1. Introduction

Globally, urban areas are expanding very quickly. Specially in developing nations the rate of urbanization is very high (Behnisch et al., 2022). Urban Sprawl is characterized by the unplanned expansion of urban area into peripheral areas (Bhatta, 2010; Pradana & Dimyati, 2024). Urban sprawl is one of the most significant effects of modernization, which is defined as the dispersed, low-density, uncontrolled growth of built-up areas into nearby natural and agricultural areas (Behnisch et al., 2022).The uncontrolled aspect of urban growth is urban sprawl. Urban sprawl is described as a phenomenon where settlements expand with low compactness and high dispersion (Behnisch et al., 2022). Urban sprawl is characterized as the rapid, unplanned expansion of cities into nearby agricultural and natural lands (Ribeiro et al., 2024). According to spatial morphology, sprawl can be categorized into two types: Leapfrog Sprawl and Linear or Ribbon Sprawl. In leapfrog sprawl, discontinuous urban patches develop beyond core urban region which creates scattered settlements patterns onto the rural land (Dewa et al., 2022). Linear or ribbon sprawl follows transportation corridors, like: roads (Zhang et al., 2023).

Land Surface Temperature measures how hot the ground actually is as detected by satellite sensors that measure heat radiation (A. Khan et al., 2021). Weather stations measures temperature of air but LST gives the actual temperature of roofs, roads, parks, and other surfaces at specific locations (Han et al., 2024). When satellite data is used to measure LST data, it is called the Surface Urban Heat Island (SUHI) (Jamarkattel et al., 2024; Li et al., 2013). The temperature difference between cities and rural areas varies throughout the day and across different seasons, usually being most intense at night

and in areas with lots of buildings and little vegetation (Melese et al., 2025). The temperature varies across the area depending on what replaces natural landscapes (Behnisch et al., 2022). When forests, farmland, and grasslands are converted to buildings, roads, and parking lots, the surface materials change completely. Natural vegetation are replaced with building materials like concrete, asphalt, and metal (Wang et al., 2018). These artificial materials have very different thermal properties. These substances reflect less sunlight. They store more heat and doesn't cool through evaporation like plants and soils (Ribeiro et al., 2024). As a result, urban areas absorb more solar energy during the day and release it slowly at night. These areas stayed warmer than vegetated areas. Higher urban temperatures create serious problems. Heat stress affects people's health (Aghamohammadi et al., 2021). Air quality worsens as higher temperatures speed up chemical reactions that create smog. Overall, thermal discomfort reduces people's willingness to spend time outdoors and decreases quality of life (Robaa, 2011).

Globally, urban sprawl increased by 95% between 1990 and 2014 (Behnisch et al., 2022). In the context of South Asia, rapid urbanization is driving significant land cover changes. As per the report of Central Bureau of Statistics Nepal (2023), urban population increased from 17.1% in 2011 to 66.8% in 2021. Studies of Nepalese cities, such as Pokhara, reveal that the expansion predominantly occurs through the conversion of agricultural land (Rai et al., 2020).

Empirical research consistently demonstrates a strong correlation between LULC changes driven by sprawl and rising LST. As cities expand, the conversion of natural lands to built-up areas leads to a steady rise in surface temperatures (F. Khan et al., 2022; Shahfahad et al., 2021). Conversely, vegetation indices (NDVI) exhibit strong negative correlations with LST. It confirms the cooling effect of green spaces (Kikon et al., 2016). Regional studies corroborate these patterns. In Pokhara, Nepal, a steady rise in LST and SUHI intensity was observed in urban areas compared to suburban zones.

The urban area in Bharatpur has grown remarkably in the past three decades. Rapid growth in built-up areas has been seen as population increases and development spreads outward. Satellite data portrays a massive increase in the built-up area of the city by almost 500% between 1990 and 2018. This makes the city one of the fastest-growing cities in Nepal (Rai et al., 2020). After 2017, the expansion of urban areas in Bharatpur accelerated as several smaller municipalities were merged together to become one metropolitan city. The urban expansion of Bharatpur city has been well documented by many researcher, it still lacks comprehensive studies that look at how Bharatpur has grown over time and what this means for local temperatures. The specific sprawl patterns in Bharatpur needs to studied closely to measure the impact of these changes on temperature. This research aims to analyze the expansion of urban growth using spatial analysis methods for year 2000 to 2020. This research is also carried out to understand the effect of land cover on Land Surface Temperature.

1.1 Study Area

Bharatpur Metropolitan City lies in Chitwan District of Bagmati Province in the south-central part of Nepal. It is situated on the eastern bank of the Narayani River. Bharatpur is surrounded by several municipalities and is well-connected to major cities across Nepal. The city is located 146 km from Kathmandu, 126 km from Pokhara, 114 km from Butwal, 128 km from Birgunj and 78 km from Hetauda. This central location has made Bharatpur an important transportation and commercial hub. The city sits at the intersection of the Mahendra Highway (East-West) and the Madan Ashrit Highway (Narayangadh- Mugling), connecting various parts of the country.

Bharatpur is the district headquarter of Chitwan District. Bharatpur is the commercial and educational hub of Chitwan as well as neighboring districts. Bharatpur is also forward in healthcare facilities. Bharatpur is characterized by relatively flat lands ideal for urbanization and agricultural land. The average elevation of Bharatpur is approximately 205m above sea level.

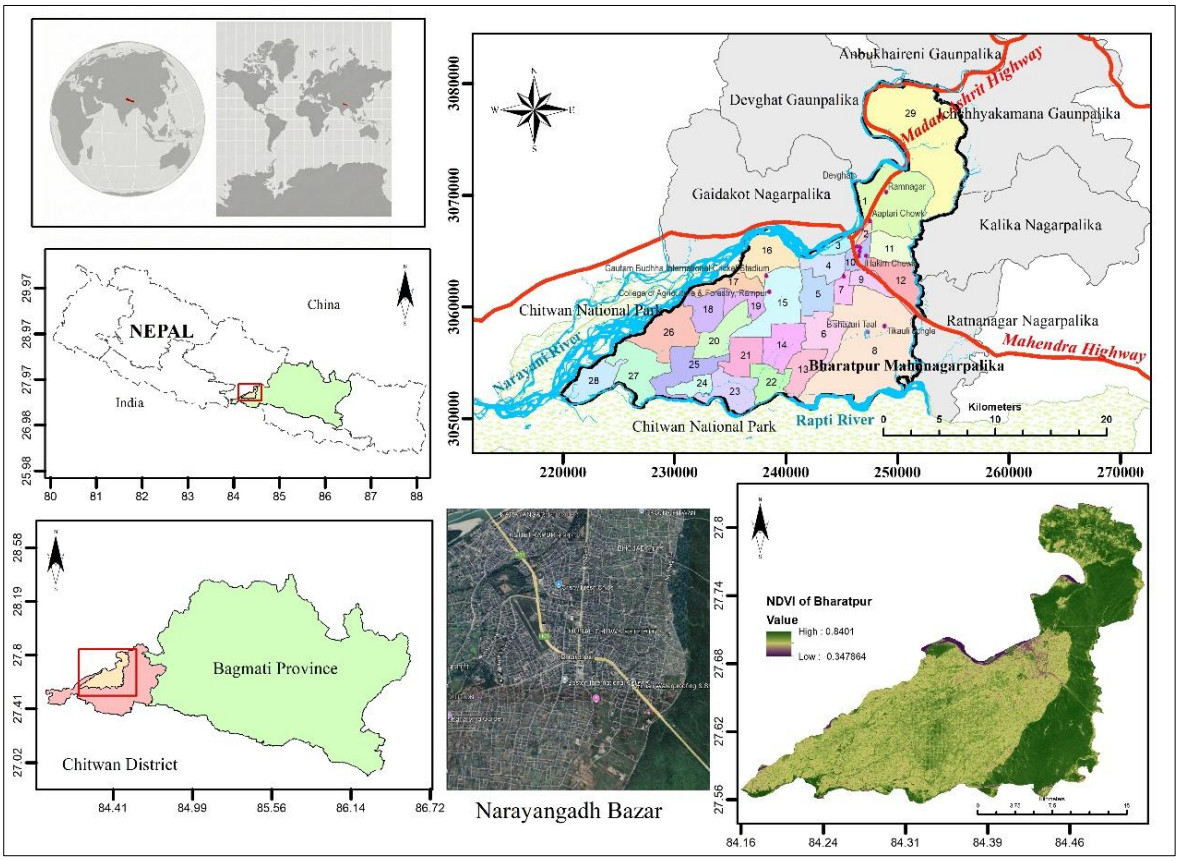

Fig. 1: Locational map of study area in Bharatpur Metropolitan City

2. Methodology

The study uses spatial techniques combined with satellite remote sensing, GIS, and statistical analysis to examine land use/land cover changes and thermal variations over a 20-year period (2000-2020). The overall methodological framework adopted for this study is illustrated in *Figure 2*. The process integrates remote sensing data acquisition, image processing, and spatial analysis to quantify urban sprawl and its thermal impacts.

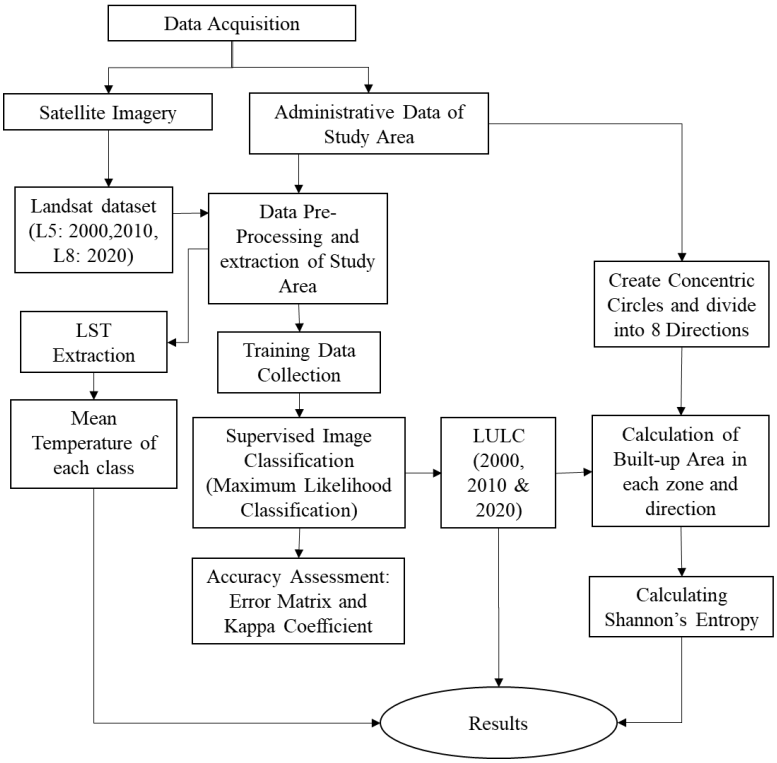

Fig. 2: The detail procedure undertaken in this study

2.1 Data Acquisition and Pre-processing

Multi-temporal satellite imagery was acquired to analyze the long-term spatial variations of the study area. Landsat 5 Thematic Mapper (TM) data were obtained for the years 2000 and 2010 and Landsat 8 OLI/TIRS data were obtained for 2020. Landsat 7 images were left from this study due to scan line error. Administrative boundary of the metropolitan was used to delineate the study area boundaries. All satellite images underwent standard pre-processing, including geometric and radiometric corrections to minimize atmospheric errors and ensure data comparability across the three time periods.

Images with WRS-2 Path 142, Row 041 that has geographic coverage of Bharatpur Metropolitan City and surrounding areas were selected for the research. Images with cloud cover between 0-10% were selected. Cloud-free or near-cloud-free imagery is essential for accurate land cover classification and surface temperature extraction (Tariq et al., 2023). Images were acquired during similar seasonal periods (preferably dry season months: November-April) to minimize seasonal variations in vegetation phenology and surface moisture that could misperceive multi-temporal comparisons. Landsat Collection 2 Level-1 Terrain Precision Corrected (L1TP) products were acquired. All spatial data processing, analysis, and visualization were conducted using ESRI ArcGIS software.

Radiometric correction was performed to normalize spectral values and remove atmospheric effects. Atmospheric effect can conceal true surface reflectance characteristics. Raw Landsat imagery is delivered as Digital Numbers (DN). It represents radiance values recorded by sensor. These values are influenced by atmospheric scattering, absorption, sensor calibration variations, and sun angle differences.

The radiometric correction workflow involved the following procedures:

(A) Conversion of Digital Numbers to Top-of-Atmosphere (TOA) Radiance

Digital Number values were first converted to at-sensor spectral radiance using sensor-specific calibration. The coefficients for the conversion are provided in the image metadata files. The metadata

files are downloaded along with the image. The conversion follows the equation:

$$L\lambda = ML \times Qcal + AL \quad (1)$$

Where:

Lλ = TOA spectral radiance (Watts/(m² × srad × μm)); ML = Band-specific multiplicative rescaling factor; Qcal = Quantized calibrated pixel value (DN); AL = Band-specific additive rescaling factor (USGS,2019)

(B) Conversion of TOA Radiance to TOA Reflectance

Radiance values were converted to TOA reflectance to adjust for variations in Earth-Sun distance as well as solar zenith angle for different image acquisition dates. This normalization allows effective comparison of imagery taken on of different dates. The conversion equation is:

$$\rho_\lambda = \frac{L\lambda}{\sin(\Theta_{SE})} \quad (2)$$

Where:

ρ_λ = TOA planetary reflectance; Θ_{SE} = Local sun elevation angle. The scene center sun elevation angle in degrees is provided in the metadata (SUN_ELEVATION); Lλ = TOA spectral radiance (USGS, 2019)

After radiometric correction all bands were stacked together to create single corrected image.

2.2 LULC Classification and Accuracy Assessment

To generate Land Use/Land Cover (LULC) maps for the years 2000, 2010, and 2020, supervised classification was used. The Maximum Likelihood Classification (MLC) algorithm was selected due to its theoretical stability and proven reliability in urban studies (Richards, 2013).

Land cover classes of Bharatpur were chosen based on the visual analysis of the Landsat images and literature review (P. Devkota et al., 2023; Rai et al., 2020). Five Land Cover classes were defined for classification; Built Up area, Forest/ Vegetation, Barren Land, Agricultural Land and Water Bodies.

Training samples were collected for all land cover classes to train the classifier. For collecting training samples, different band compositions were used for image analysis. Various band combinations help to analyze the land cover classes effectively because of the varying spectral behavior of the land cover classes. False color composites exploit the human eyes sensitivity to color variation (Lillesand et al., 2015).

Classification accuracy assessment ensures the agreement between classified maps and reference data. It provides essential quality control for land cover products (Congalton & Green, 2019). Without rigorous accuracy assessment, the reliability of analysis and interpretation remains unknown. Post-classification, the accuracy of the LULC maps was evaluated using an Error Matrix, from which the Overall Accuracy and Kappa Coefficient were calculated to validate the results.

A subset was created from the training samples collected for supervised calculation. 20% of the original training samples were used for accuracy assessment of the classified map and the remaining 80% of the training sample was used for classification.

2.3 Urban Sprawl Analysis using Shannon's Entropy

To quantify the degree of urban sprawl and spatial dispersion, Shannon's Entropy ($\boldsymbol{H_n}$) was computed for the years 2000, 2010, and 2020. This metric evaluates whether land development is concentrated (compact) or dispersed (sprawl) relative to the urban core (Yeh & Li, 2001).

Chaubishkothi Chowk was identified as the Central Business District (CBD) and designated as the center point for analysis due to its established role as the city's primary commercial and administrative hub. A multi-directional gradient analysis was performed in ArcGIS using the following spatial constraints:

Concentric Buffers Rings were generated at 2-km intervals radiating from the CBD up to 30

km (15 rings) (Bhatta, 2010). The area was divided into eight cardinal and inter-cardinal sectors (N, NE, E, SE, S, SW, W, NW) of 45° each.The intersection of these buffers and sectors created a grid. Zones falling outside the metropolitan boundary were excluded, resulting in a consistent set of n = 61 zones for all temporal periods.

(A) Calculation and Interpretation

For each zone, the quantity of built-up area was extracted using zonal statistics. Shannon's Entropy (***H***)was calculated as:

$$H = - \Sigma(Pi \times \ln(Pi)) \quad (3)$$

Where:

H = Shannon entropy value

Pi = Proportion of built-up area in zone i (calculated as: built-up area in zone i / total built-up area across all zones)

Σ = Summation across all n zones (Mhangara et al., 2024)

To standardize the results for temporal comparison, the value was normalized to derive Relative Entropy ($\boldsymbol{H_n}$):

$$H_n = \frac{H}{ln(n)} \quad (4)$$

The value of $\boldsymbol{H_n}$ranges from 0 to 1. The interpretation of the entropy values is detailed in Table 1 (Das & Angadi, 2021).

Table 1: Interpretation of Relative Entropy $\boldsymbol{H_n}$

Relative Entropy ($\boldsymbol{H_n}$)	**Classification**	**Characteristics**
0.0 – 0.3	Highly Compact	Development concentrated near CBD.
0.3 – 0.5	Moderately Compact	Emerging peripheral growth.
> 0.5	Sprawl	Dispersed development (Threshold for Sprawl).
0.8 – 1.0	Extreme Sprawl	Highly fragmented, uniform dispersion.

An increase in $\boldsymbol{H_n}$over time indicates a shift toward dispersed urban sprawl, while a decrease suggests infill development and compaction.

2.4 Land Surface Temperature (LST) Extraction

LST was derived using Google Earth Engine (GEE). LST retrieval was performed using the thermal infrared bands of the Landsat datasets. The study utilized Top-of-Atmosphere (TOA) reflectance collections clipped to the administrative boundary of Bharatpur Metropolitan City. The digital numbers (DN) were converted to top-of-atmosphere (TOA) spectral radiance and subsequently to brightness temperature.

To ensure temporal consistency between Land Use Land Cover (LULC) and thermal analysis, Landsat imagery was acquired for three decadal periods: 2000, 2010, and 2020. A "Multi-Year Seasonal Stacking" technique was employed to mitigate cloud cover and ensure sufficient data availability (Ermida et al., 2020). Images were restricted to the pre-monsoon and monsoon seasons (April to August) to capture consistent thermal characteristics.

The specific sensor selection and temporal aggregation were as follows:

2000: Landsat 7 ETM+ (aggregated 2000–2003).

2010: Landsat 5 TM (aggregated 2009–2011).

2020: Landsat 8 TIRS (aggregated 2020–2023).

Landsat 5 was selected over Landsat 7 for this period to avoid data gaps and radiometric instability caused by the SLC failure in Landsat 7 (Markham et al., 2012). All images were filtered to WRS Path 142. Cloud and cloud shadow masking were rigorously applied using the QA_PIXEL quality assessment band (Bits 3 and 4) to retain only clear-sky pixels. LST was derived using a single-channel algorithm that corrects for emissivity. The process involved the following sequential steps:

(A) NDVI and Vegetation Proportion (P_v)

Normalized Difference Vegetation Index (NDVI) was calculated to estimate the proportion of vegetation (P_v) per pixel, following the method by (Sobrino et al., 2004):

$$P_v = \frac{NDVI - 0.2}{(0.5-0.2)^2} \quad (5)$$

This formula assumes that NDVI values below 0.2 represent bare soil with no vegetation. NDVI values above 0.5 represent full vegetation cover (Sobrino et al., 2004). The squared term creates a non-linear relationship that represents actual vegetation proportions.

(B) Land Surface Emissivity (ε)

Surface emissivity was calculated based on P_v applying a threshold method suitable for mixed urban-agricultural landscapes (Sobrino et al., 2004) :

$$\varepsilon = 0.004 \times P_v + 0.986 \quad (6)$$

(C) Conversion to LST

Satellite brightness temperature (BT) was converted to emissivity-corrected LST (in Celsius) using the inversion of Planck's law (Sajib & Wang, 2020):

$$LST = \frac{BT}{1 + \lambda \times {}^{BT}/_{\rho} \times \ln(\varepsilon)} - 273.15 \quad (7)$$

Where:

BT = Brightness temperature from thermal band (in Kelvin)

λ = Wavelength of emitted radiance (11.45 μm for Landsat 5/7 and 10.895 for Landsat 8)

ρ = h × c / σ = 1.438 × 10^{-2} m·K (Planck's constant related value)

ε = Land surface emissivity

273.15 = Conversion from Kelvin to Celsius

Final LST maps for each epoch were generated using a median compositing function to minimize outliers and seasonal variability.

The overall annual mean LST was computed using the zonal statistics of the entire study area, representing an area-weighted mean of the contributing LULC classes.

4. Results and Discussion

The accuracy assessment was carried out for classified maps of all years (2000, 2010 and 2020) using the 20% of random training samples. The LULC map of 2000 had Overall Accuracy (OA) of 96.41% with Kappa Coefficient of 94%. For year 2010, OA is 95.83% and Kappa Coefficient is 92.37%. Similarly, for year 2020, the OA is 93.91% and Kappa Coefficient is 89.83%. These values substantially exceed the minimum acceptable thresholds of 85% overall accuracy and 0.80 kappa coefficient recommended for land cover mapping (Feizizadeh et al., 2022; Lillesand et al., 2015). These classified maps were then used for further analysis.

4.1 LULC Distribution and Changes

The analysis of LULC changes in Bharatpur Metropolitan City over the two-decade study period (2000–2020) reveals significant transformations in the urban landscape. The Landsat images were preprocessed for radiometric correction using equation (1) and equation (2). The processed images were stacked together using mosaic tool in ArcMAP. Throughout the study period, agricultural land

remained the dominant land cover class, though it experienced a steady decline. In 2000, agricultural land covered 242.14 km² (55.92%) of the city, but this decreased to 223.16 km² (51.54%) by 2020. This represents a net loss of 18.98 km² (-7.84%). The land cover class is the most severely impacted by land conversion. Forest/Vegetation class was the second largest category. It also showed a downward trend. It decreased from 178.69 km² (41.27%) in 2000 to 170.08 km² (39.28%) in 2020. This results in a net loss of 8.61 km² (-4.82%). The rate of forest loss accelerated in the second decade, with a loss of 6.05 km² between 2010 and 2020 compared to 2.56 km² in the preceding decade.

The most considerable change was observed in the Built-Up area. The land cover class exhibited exponential growth. Starting from a small 1.53 km² (0.35%) in 2000, the built-up area surged to 30.02 km² (6.93%) by 2020. This shows a massive net increase of 28.49 km², representing a +1,862% growth over 20 years. The expansion was particularly aggressive between 2010 and 2020, where the built-up area more than tripled, adding 21.10 km² in just ten years.

Minor land cover classes showed mixed trends. Water Bodies increased by 2.37 km² (+79.3%), growing from 0.69% to 1.24% of the total area. Conversely, Barren land fluctuated, peaking in 2010 before declining to 4.37 km² (1.01%) by 2020, resulting in a net decrease of 42.9%.

Table 2: LULC Area Distribution and Net Change Analysis (2000–2020)

Land Cover Class	2000 Area (km²)	%	2010 Area (km²)	%	2020 Area (km²)	%	Net Change 2000–2020 (km²)	Net Change (%)
Agriculture	242.14	55.92	234.96	54.26	223.16	51.54	-18.98	-7.84
Forest/Vegetation	178.69	41.27	176.13	40.68	170.08	39.28	-8.61	-4.82
Built-Up	1.53	0.35	8.92	2.06	30.02	6.93	+28.49	+1,862
Water Bodies	2.99	0.69	4.55	1.05	5.36	1.24	+2.37	+79.3
Barren	7.66	1.77	8.23	1.90	4.37	1.01	-3.29	-42.9
Total	**433.01**	**100.0**	**433.01**	**100.0**	**433.01**	**100.0**	-	-

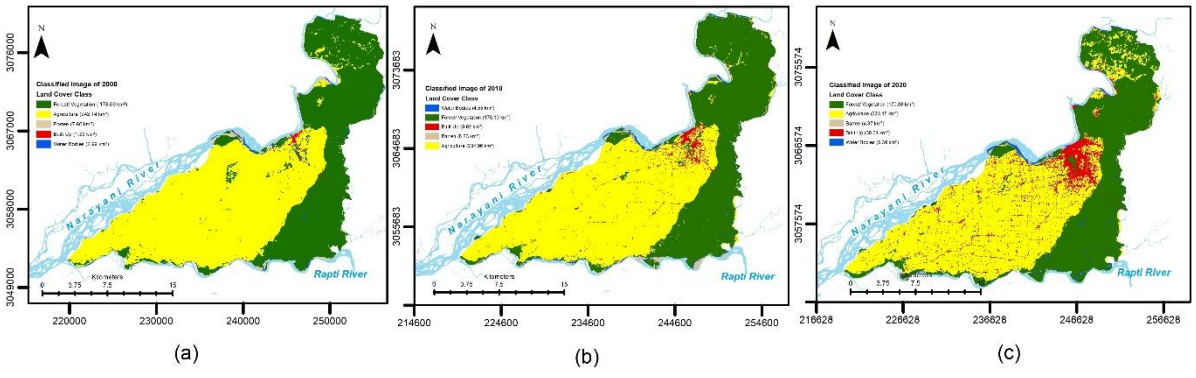

Fig. 3: Classified maps of Bharatpur Metropolitan City for years: (a) 2000, (b) 2010 and (c) 2020

4.2 Shannon's Entropy

Shannon's entropy was calculated to quantify the spatial dispersion of built-up areas relative to the Central Business District (CBD) at Chaubishkothi. The results demonstrate a clear transition from a moderately compact urban form to a highly dispersed, sprawling pattern over the 20-year study period.

Table 3 presents the absolute entropy ($\boldsymbol{H}$), relative entropy ($\boldsymbol{H_n}$), and the corresponding sprawl classification for each temporal point.

Table 3: Shannon's Entropy Results (2000–2020)

Year	Shannon's Entropy (H)	Relative Entropy (H_n)	Sprawl Classification
2000	2.32	**0.56**	Moderate Dispersion
2010	3.35	**0.81**	High Sprawl
2020	3.60	**0.88**	Extreme Sprawl

In 2000, the relative entropy value was $\boldsymbol{H_n}$ = 0.56. Although this value slightly exceeded the 0.5 threshold typically marking the onset of sprawl (Das & Angadi, 2021). It indicated a Moderately Dispersed pattern. At this stage, built-up areas were largely concentrated within zones closer to the CBD, though early signs of "leapfrog" development were already detectable in the periphery.

By 2010, a significant shift in urban form occurred. The relative entropy rose sharply by 0.25 units to reach $\boldsymbol{H_n}$ = 0.81, representing a 44.6% increase in dispersion. This value crossed the critical threshold into the High Sprawl classification. This drastic rise signals that the decade from 2000 to 2010 was the primary acceleration period for urban scattering, where development ceased to be contiguous with the core and began spreading extensively across the metropolitan grid.

In 2020, the trend continued with relative entropy reaching $\boldsymbol{H_n}$= 0.88, classifying the city's development pattern as Extreme Sprawl. An entropy value approaching 1.0 indicates that built-up land is distributed almost uniformly across all available zones rather than being concentrated in specific urban clusters. This statistical finding aligns with spatial observations of development extending up to 30 km from the CBD, particularly in the southwestern regions.

The consistent upward trajectory of entropy values confirms that Bharatpur is expanding through a fragmented, non-contiguous pattern rather than through densification or infilling. The high value of 0.88 in 2020 suggests that the city's footprint has become nearly as random and dispersed as theoretically possible within the defined spatial zones.

4.3 Land Surface Temperature

The mean LST of the study area fluctuated over the observation period. The LST decreased from 30.21°C in 2000 to 27.18°C in 2010, before stabilizing at 27.55°C in 2020. These changes are likely due to year-to-year weather differences or changes in satellite sensors, rather than a single long-term cooling trend. Despite this overall fluctuation, a critical shift occurred in the thermal ranking of land cover classes. In 2000, agricultural land was the warmest category (31.92°C). Likely due to spatial coverage. However, by 2020, built-up areas emerged as the dominant heat source, recording the highest mean temperature of 29.10°C and surpassing all other categories. This transition highlights a widening thermal gap between urban and natural surfaces. In 2020, built-up areas were approximately 3°C warmer than forest cover (26.13°C) and 3.6°C warmer than water bodies (25.52°C). This distinct gradient confirms that as the city has expanded, impervious surfaces are significantly intensifying the local thermal environment relative to the natural surroundings. Table 4 shows the overall mean temperature for each year represents the area-weighted mean of the entire study region, accounting for the varying pixel counts of each LULC class.

Table 4: Mean LST by Land Use/Land Cover Class (°C)

LULC Class	2000	2010	2020	Change (2000-2020)	Rank 2020
Mean Temperature	30.21	27.18	27.55		
Built-Up	30.37	29.86	29.10	-1.27	1 (Hottest)

Agriculture	31.92	28.13	27.94	-3.98	3
Barren	30.76	27.99	27.48	-3.28	2
Forest/Vegetation	27.94	26.28	26.13	-1.81	4
Water Bodies	26.40	26.03	25.52	-0.88	5 (Coolest)

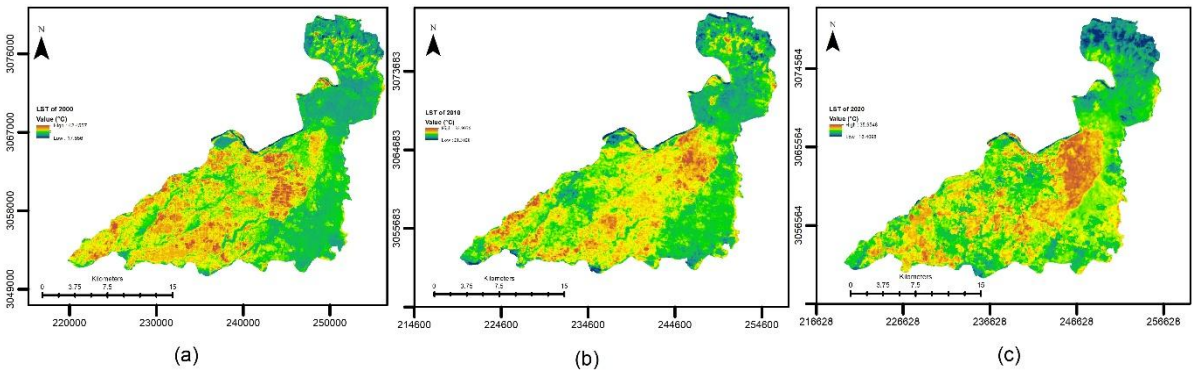

Fig. 4: LST Maps of Bharatpur Metropolitan City for year (a) 2000, (b) 2010 and (c) 2020

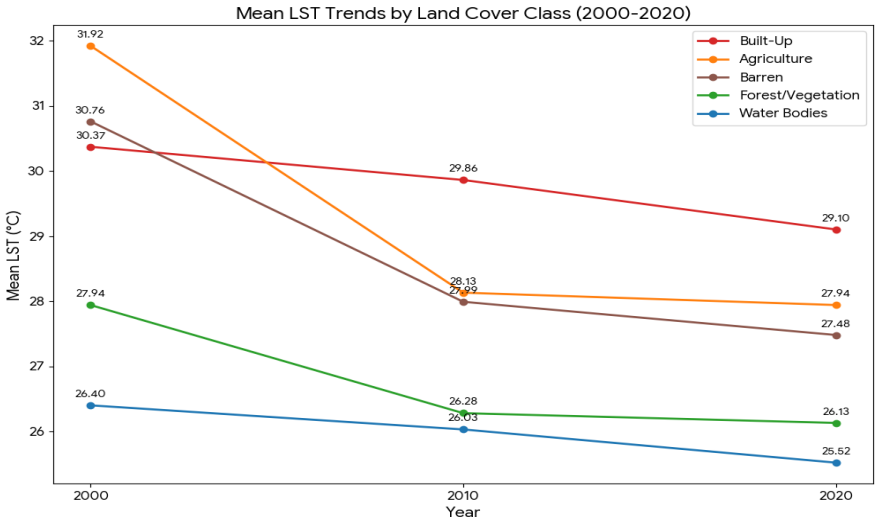

Fig. 5: Variation of mean LST by land cover within the study period (2000-2020)

4.4 Discussion

The analysis of the last two decades reveals that Bharatpur Metropolitan City is undergoing a transformation characterized not only by growth, but by aggressive urban sprawl. The LULC data highlights a dramatic expansion in the built-up area, which surged from 1.5 km² in 2000 to 30.0 km² by 2020. This massive expansion comes from the expense of agricultural and forest lands primarily.

(Rai et al., 2020) performed satellite based analysis on driving factors causing urban expansion on Pokhara and Bharatpur Metropolitan City. They have found in their study that the increase in urban population and internal migration are the major causes of urban expansion. As per Nation Census Report of 2068 (2011), the population of Bharatpur Municipality was 280,502 with population density of 665.10 person km^2. In Census 2078, population growth rate was recorded 2.68% per year and the total population of Bhatarpur Metropolitan city reached to 369268 with population density of 853person/ km^2. The growing population of the metropolitan city is the cause of expansion of built up area. (Central Bureau of Statistics, 1995; CBS,2021). 1n 1960, measures were taken to eradicate Malaria from the

terai region. The flat lands of Terai have attracted huge number people for settlement in 1970's and 1980's (Rai et al., 2020; K. Devkota, 2012). This increased the urbanization pressure in the terai region (Rai et al., 2020). The settlement has increased around East – West Highway (K. Devkota, 2012). (P. Devkota et al., 2023) in their study of 12 rapidly urbanizing city of Nepal also assessed the urban expansion of Bharatpur Metropolitan City. Bharatpur have also attracted lots of migration after its conversion into metropolitan city.

Remote sensing and GIS was used for mapping LULC of Simly watershed of Pakistan (Butt et al., 2015). The research showed the as settlement areas have increased the area of watershed has been reduced. In Bharatpur, the combined reduction in agricultural and forest land (~27.6 km²) closely matches the built-up increase (~28.5 km²), suggesting that urban expansion primarily replaced these two land categories. This reflects typical peri-urban development patterns observed in rapidly growing South Asian cities.

Shannon's Entropy confirms that this growth is disorganized "sprawl" rather than planned, compact development. Entropy measures how "spread out" a city is. If a city grows neatly around a center, the value stays low. Dhali et al., (2019)'s studied urban growth on The North 24 Paragnas District of West Bengal, India for year 1989, 2006 and 2016. The built up area in the region was found to be distributed throughout the district especially on the west side due to influence of the Kolkatta City. This study highlighted the sprawl among the urban centers of the district (Dhali et al., 2019). (Das & Angadi, 2021) on their temporal study of LULC of municipalities in Barrackpore Subdivision of West Bengal, found that the area of built up area was constantly increasing in the expense of area of agricultural land, vegetation and water bodies. The relative Shannon's entropy of the municipal areas were near to 1 showing extreme sprawl in the municipality areas (Das & Angadi, 2021). In the case of Bharatpur, the entropy value shot up from roughly 0.56 in 2000 to a very high 0.88 in 2020. Since the value is getting very close to 1 (the maximum), it is strong statistical proof that the city is expanding in a scattered, chaotic way across the landscape. Similarly, in Indian cities like Bengaluru, a doubling of built-up area was associated with significant increases in mean LST (Keerthi Naidu & Chundeli, 2023). Research in Turkey projected that the decline of natural lands and their replacement by urban areas would inevitably increase provincial temperatures (Ergen, 2025).

Meteorological records for Nepal show that 2000 was a year of significant moisture deficits and drought-like conditions across the Terai region. Research by Sigdel & Ikeda, (2010) confirms that the pre-monsoon season of 2000 saw below-average rainfall and high aridity (Sigdel & Ikeda, 2010). Furthermore, regional monitoring identified 2000 as a "non-El Niño" year, which is often associated with reduced soil moisture in the Indo-Gangetic plains (Bagale et al., 2021). This regional dryness likely spiked the surface temperatures of the agricultural areas. Dry, bare soil heats up much faster than moist soil. It is a process known as climatic forcing. The high mean temperature in 2000 in Bharatpur reflects a regional weather event rather than the urban heat island effect. By 2010 and 2020, although the city core was getting hotter due to urbanization, the surrounding rural areas likely returned to more typical moisture levels, which pulled the overall regional average down.

Assessment of LULC and LST in Bengalaru, India using Landsat images based classification showed 50% of vegetation has been lost in years between 2000 to 2021 (Keerthi Naidu & Chundeli, 2023). In the same time period the area of built up area surged higher. The mean LST of city was increased by 3 degree Celsius from 26°C to 29°C in 2021. Bharatpur is also experiencing similar trend. The mean temperature of built up region went on increasing as its spatial coverage increased with time.

5. Conclusion

This study assessed the impact of urban sprawl on Land Surface Temperature (LST) in Bharatpur Metropolitan City over the study period (2000–2020). The research highlights a link between

rapid urbanization and changing thermal patterns in the city, by integrating LULC mapping, Shannon's Entropy and LST analysis.

The most significant finding of this research is expansion of the built-up area. Between 2000 and 2020, the built-up area grew from just 1.53 km² to 30.02 km². This growth came largely with the depletion of agricultural land and vegetation. The decline of agricultural land was notable during the same period. The Shannon's Entropy analysis confirms that this growth was not only rapid but also highly disorganized. The relative entropy value rose from 0.56 (Moderate Dispersion) in 2000 to 0.88 in 2020. The Shannon's Entropy value classifies the city's current expansion as "Extreme Sprawl".
(Belay et al., 2025) study suggested maintaining and restoring vegetation cover is critical for regulating the microclimate in the Ethiopian Highlands. They suggest that sustainable land management practices and afforestation are essential strategies to mitigate rising temperatures and protect the hydrological balance of the Nile basin.

The rapid and unplanned urban expansion is altering microclimate of Bharatpur Metropolitan City. Although, the metropolitan city still has higher area of agricultural lands, urban sprawl is dominating the metropolitan city. The unplanned development is spreading over the agricultural land. The disorganized sprawl disrupts the natural harmony and ecological balance of the city. The urban area is the constant contributor for driving up the local temperature.

Acknowledgement

The authors would like to express their sincere gratitude to Pashchimanchal Campus, Department of Geomatics Engineering for providing the necessary academic environment and support to conduct this research. We are deeply thankful to Er. Umesh Bhurtel, Er. Netra Katuwal, Er. Saurav Gautam and Er. Pradip Aryal for their great assistance, technical insights, and unwavering support throughout the study. We also extend our thanks to our friends and colleagues for their encouragement and help.

We acknowledge the United States Geological Survey (USGS) for making the Landsat archive data publicly available and Google Earth Engine (GEE) for providing the high-performance cloud computing platform that facilitated the processing of multi-temporal satellite imagery. Finally, we thank the developers of the GIS software used for the spatial analysis and visualization presented in this work.

References

Aghamohammadi, N., Fong, C. S., Idrus, M. H. M., Ramakreshnan, L., & Sulaiman, N. M. (2021). Environmental heat-related health symptoms among community in a tropical city. *Science of the Total Environment, 782*, 146611. https://doi.org/10.1016/j.scitotenv.2021.146611

Behnisch, M., Krüger, T., & Jaeger, J. A. G. (2022). Rapid rise in urban sprawl: Global hotspots and trends since 1990. *PLOS Sustainability and Transformation*, *1*(11 November), 1–30. https://doi.org/10.1371/journal.pstr.0000034

Belay, T., Melese, T., & Terefe, B. (2025). Spatio-temporal dynamics of vegetation cover and land surface temperature in the North Gojjam sub-basin, Ethiopia. *Discover Applied Sciences*, *7*(12). https://doi.org/10.1007/s42452-025-07941-y

Bhatta, B. (2010). *Analysis of Urban Growth and Sprawl from Remote Sensing Data.pdf* (1st ed.). Springer Berlin, Heidelberg. https://doi.org/10.1007/978-3-642-05299-6

Butt, A., Shabbir, R., Ahmad, S. S., & Aziz, N. (2015). Land use change mapping and analysis using

Remote Sensing and GIS: A case study of Simly watershed, Islamabad, Pakistan. *Egyptian Journal of Remote Sensing and Space Science*, *18*(2), 251–259. https://doi.org/10.1016/j.ejrs.2015.07.003

Central Bureau of Statistics. (1995). *Population Monograph of Nepal 1995*. https://www.academia.edu/download/37235139/Nepal_Population_Monograph_2014_volume2.pdf

Congalton, R. G., & Green, K. (2019). *Assessing the Accuracy of Remotely Sensed Data*. CRC Press. https://doi.org/10.1201/9780429052729

Das, S., & Angadi, D. P. (2021). Assessment of urban sprawl using landscape metrics and Shannon's entropy model approach in town level of Barrackpore sub-divisional region, India. *Modeling Earth Systems and Environment*, *7*(2), 1071–1095. https://doi.org/10.1007/s40808-020-00990-9

Devkota, K. (2012). Dynamics of Urbanization in Nepal : The Role and Response of Local Government. *Alliance for Social Dialouge POlicy Research Fellowship Program*, *December*.

Devkota, P., Dhakal, S., Shrestha, S., & Shrestha, U. B. (2023). Land use land cover changes in the major cities of Nepal from 1990 to 2020. *Environmental and Sustainability Indicators*, *17*(December 2022), 100227. https://doi.org/10.1016/j.indic.2023.100227

Dewa, D. D., Buchori, I., Sejati, A. W., & Liu, Y. (2022). Shannon Entropy-based urban spatial fragmentation to ensure sustainable development of the urban coastal city: A case study of Semarang, Indonesia. *Remote Sensing Applications: Society and Environment*, *28*, 100839. https://doi.org/10.1016/j.rsase.2022.100839

Dhali, M. K., Chakraborty, M., & Sahana, M. (2019). Assessing spatio-temporal growth of urban sub-centre using Shannon's entropy model and principle component analysis: A case from North 24 Parganas, lower Ganga River Basin, India. *Egyptian Journal of Remote Sensing and Space Science*, *22*(1), 25–35. https://doi.org/10.1016/j.ejrs.2018.02.002

Ergen, M. (2025). Spatıotemporal analysıs of urban development and land USE in sakarya provınce, Türkiye: ımplıcatıons for future urban growth modelıng. *GeoJournal*, *90*(3), 112. https://doi.org/10.1007/s10708-025-11363-z

Ermida, S. L., Soares, P., Mantas, V., Göttsche, F. M., & Trigo, I. F. (2020). Google earth engine open-source code for land surface temperature estimation from the landsat series. *Remote Sensing*, *12*(9), 1–21. https://doi.org/10.3390/RS12091471

Feizizadeh, B., Darabi, S., Blaschke, T., & Lakes, T. (2022). QADI as a New Method and Alternative to Kappa for Accuracy Assessment of Remote Sensing-Based Image Classification. *Sensors*, *22*(12), 1–21. https://doi.org/10.3390/s22124506

Han, D., Cai, H., Wang, F., Wang, M., Xu, X., Qiao, Z., An, H., Liu, Y., Jia, K., Sun, Z., & Wang, S. (2024). Understanding the role of urban features in land surface temperature at the block scale: A diurnal cycle perspective. *Sustainable Cities and Society*, *111*, 105588. https://doi.org/10.1016/j.scs.2024.105588

Jamarkattel, U., Sherchan, B., & K C, N. (2024). Measuring Urban Heat Islands in Metropolitan City, Pokhara, Using Remote Sensing. *Journal of Engineering and Sciences*, *3*(2), 73–80. https://doi.org/10.3126/jes2.v3i2.72192

Keerthi Naidu, B. N., & Chundeli, F. A. (2023). Assessing LULC changes and LST through NDVI and NDBI spatial indicators: a case of Bengaluru, India. *GeoJournal*, *88*(4), 4335–4350. https://doi.org/10.1007/s10708-023-10862-1

Khan, A., Chatterjee, S., & Weng, Y. (2021). Characterizing thermal fields and evaluating UHI effects. In *Urban Heat Island Modeling for Tropical Climates* (pp. 37–67). Elsevier. https://doi.org/10.1016/B978-0-12-819669-4.00002-7

Khan, F., Das, B., & Mohammad, P. (2022). *Urban Growth Modeling and Prediction of Land Use Land Cover Change Over Nagpur City, India Using Cellular Automata Approach* (pp. 261–282). https://doi.org/10.1007/978-981-16-7373-3_13

Kikon, N., Singh, P., Singh, S. K., & Vyas, A. (2016). Assessment of urban heat islands (UHI) of Noida City, India using multi-temporal satellite data. *Sustainable Cities and Society*, *22*, 19–28. https://doi.org/10.1016/j.scs.2016.01.005

Li, X., Zhou, W., & Ouyang, Z. (2013). Relationship between land surface temperature and spatial pattern of greenspace: What are the effects of spatial resolution? *Landscape and Urban Planning*, *114*, 1–8. https://doi.org/10.1016/j.landurbplan.2013.02.005

Lillesand, T., Kiefer, R. W., & Chipman, J. (2015). *Remote sensing and image interpretationo Title* (Seventh Ed). https://books.google.com.np/books?hl=en&lr=&id=AFHDCAAAQBAJ&oi=fnd&pg=PR12&dq=remote+sensing+and+image+interpretation&ots=0Etsj_aAds&sig=0PHLuVcSsVjBEnbD40_W5TPgMpk&redir_esc=y#v=onepage&q=remote sensing and image interpretation&f=false

Markham, B. L., Haque, M. O., Barsi, J. A., Micijevic, E., Helder, D. L., Thome, K. J., Aaron, D., & Czapla-Myers, J. S. (2012). Landsat-7 ETM+: 12 years on-orbit reflective-band radiometric performance. *IEEE Transactions on Geoscience and Remote Sensing*, *50*(5 PART 2), 2056–2062. https://doi.org/10.1109/TGRS.2011.2169803

Melese, M., Anteneh, M., & Bantigegn, S. (2025). Urbanization and land surface temperature dynamics in Bahir Dar, Ethiopia: a comparative analysis of pre- and post-capital status. *Frontiers in Environmental Science*, *13*(April), 1–18. https://doi.org/10.3389/fenvs.2025.1569636

Mhangara, P., Gidey, E., & Manjoo, R. (2024). Analysis of urban sprawl dynamics using machine learning, CA-Markov chain, and the Shannon entropy model: a case study in Mbombela City, South Africa. *Environmental Systems Research*, *13*(1). https://doi.org/10.1186/s40068-024-00348-5

Pradana, M. R., & Dimyati, M. (2024). Tracking Urban Sprawl: A Systematic Review and Bibliometric Analysis of Spatio-Temporal Patterns Using Remote Sensing and GIS. *European Journal of Geography*, *15*(3), 190–203. https://doi.org/10.48088/ejg.m.pra.15.3.190.203

Rai, R., Yili, Z., Paudel, B., Khanal, N. R., & Acharya, B. K. (2020). Satellite Image-Based Monitoring of Urban Land Use Change and Assessing the Driving Factors in Pokhara and Bharatpur Metropolitan Cities, Gandaki Basin, Nepal. *Journal of Resources and Ecology*, *11*(1), 87. https://doi.org/10.5814/j.issn.1674-764x.2020.01.009

Ribeiro, M. P., Menezes, G. P., Figueiredo, G. K. D. A., de Mello, K., & Valente, R. A. (2024). Impacts of urban landscape pattern changes on land surface temperature in Southeast Brazil. *Remote Sensing Applications: Society and Environment*, *33*, 101142. https://doi.org/10.1016/j.rsase.2024.101142

Richards, J. A. (2013). Supervised Classification Techniques. In *Remote Sensing Digital Image Analysis* (pp. 247–318). Springer Berlin Heidelberg. https://doi.org/10.1007/978-3-642-30062-2_8

Robaa, S. M. (2011). Effect of urbanization and industrialization processes on outdoor thermal human comfort in Egypt. *International Journal of Meteorology*, *36*(360), 111–125. https://doi.org/10.4236/acs.2011.13012

Sajib, M. Q. U., & Wang, T. (2020). Estimation of land surface temperature in an agricultural region of Bangladesh from landsat 8: Intercomparison of four algorithms. *Sensors (Switzerland)*, *20*(6). https://doi.org/10.3390/s20061778

Shahfahad, Rihan, M., Naikoo, M. W., Ali, M. A., Usmani, T. M., & Rahman, A. (2021). Urban Heat Island Dynamics in Response to Land-Use/Land-Cover Change in the Coastal City of Mumbai. *Journal of the Indian Society of Remote Sensing*, *49*(9), 2227–2247. https://doi.org/10.1007/s12524-021-01394-7

Sobrino, J. A., Jiménez-Muñoz, J. C., & Paolini, L. (2004). Land surface temperature retrieval from LANDSAT TM 5. *Remote Sensing of Environment*, *90*(4), 434–440. https://doi.org/10.1016/j.rse.2004.02.003

Tariq, A., Mumtaz, F., Majeed, M., & Zeng, X. (2023). Spatio-temporal assessment of land use land cover based on trajectories and cellular automata Markov modelling and its impact on land surface temperature of Lahore district Pakistan. *Environmental Monitoring and Assessment*, *195*(1), 114. https://doi.org/10.1007/s10661-022-10738-w

USGS. (2019). *Landsat 4-7 surface reflectance code (LaSRC) product guide* (Version 3.0). U.S. Geological Survey.

Wang, C., Wang, Z. H., & Yang, J. (2018). Cooling Effect of Urban Trees on the Built Environment of Contiguous United States. *Earth's Future*, *6*(8), 1066–1081. https://doi.org/10.1029/2018EF000891

Yeh, A., & Li, X. (2001). Measurement and monitoring of urban sprawl in a rapidly growing region using entropy. *American Society for Photogrammetry and Remote Sensing*, *Photogrammetric Engineering And Remote Sensing*. http://www.asprs.org/publications/pers

Zhang, L., Shu, X., & Zhang, L. (2023). Urban Sprawl and Its Multidimensional and Multiscale Measurement. *Land*, *12*(3), 1–17. https://doi.org/10.3390/land12030630